

APPLICATION OF ARTIFICIAL NEURAL NETWORK IN THE APS LINAC BUNCH CHARGE TRANSMISSION EFFICIENCY*

H. Shang[†], Y. Sun, R. Maulik, Argonne National Laboratory, Argonne, USA
T. Xu, Northern Illinois University, Department of Physics, DeKalb, USA

Abstract

In recent years there has been a rapid growth in machine learning (ML) and artificial intelligence (AI) applications in accelerators [1]. Tools based on ML can help substantially in revealing co-relations of machine conditions and beam parameters that are not easily discovered using traditional model-based simulations. Reducing machine tuning time is among the many possible applications. While at APS, we have many conventional tools for the optimization, diagnostics, and controls of the accelerators, we would like to explore and test ML-based methodologies for APS machine operation, optimization, and control. In this paper, an application of neural networks to the APS linac bunch charge transmission efficiency is presented.

INTRODUCTION

The APS linac [2,3] has been designed for static operating conditions: beam energy, beam current, bunch lengths, and bunch charge. Recently, interleaving operation [4, 5] was introduced to the APS linac requiring switching the linac every two minutes between two modes of operation. After the APS Upgrade [6] is complete, switching will need to be done every 5 to 10 seconds [7]. The performance of the APS linac will need to be pushed beyond its current state-of-the-art for a planned demonstration of a high efficiency FEL [8] in the APS linac extension area. Reaching these goals will be extremely challenging and time consuming, if possible at all, with a manual machine tune up. In addition, the dynamics of intense electron bunches in linear accelerators like the APS linac are dominated by complex collective effects, such as wakefields, space charge, and coherent synchrotron radiation [9], that are not very predictable, making it difficult to control and tune beam properties using model-based approaches. Application of machine learning is extremely well-suited to accelerators with their ability to produce vast data sets using a high repetition rate of beam pulses.

The objective of our approach is to establish and test three ML models at the APS linac to speed up processing of the rf gun front-end charge optimization. The bunch charge measured after the chicane via a current monitor (L3:CM1 charge) is shown in Fig. 1. Sixteen variables are included in the ML-based models. These are bipolar power supplies for magnets installed between the thermionic rf gun [10] and the first accelerating structure, consisting of seven quadrupoles and nine steering magnets.

* Work supported by the U.S. Department of Energy, Office of Science, under Contract No. DE-AC02-06CH11357.

[†] shang@anl.gov

NEURAL NETWORK MODEL

Three standard neural network (NN) models were built, each consisting of an input layer, two or three hidden layers, and an output layer. The models are:

- NNN: with 3 hidden layers, and the numbers of nodes in the hidden layers are 128, 256, and 256.
- NNN64: with 3 hidden layers, and the number of nodes in each hidden layer is 64.
- NN64: with 2 hidden layers, and the number of nodes in each hidden layer is 64. It is the same as NNN64 but with one fewer hidden layer.

The difference between the three NN models is in the hidden layers. With a small data set of 2000 data points and using the number of hidden layers and the number of nodes in each hidden layer, a parallel optimization method determined that the best NN model found by a parallel optimization method is the model with three hidden layers and 75 nodes in each layer. This 75-node 3-hidden-layer NN model on the complete data set shows no obvious difference from the NNN64 model, so NNN64 is chosen for study. Further optimization with the complete data set is not necessary, since these models produce satisfactory results. This is fortunate, as optimization with the full data set would be time consuming and resource intensive.

DATA PREPARATION

Operational data archived from the past two years by the APS data logger were used to train the ML model. Data with a 4-second interval was chosen. To avoid the read-back noise, we used the setpoints of the magnets. As with the optimization [11], 16 magnets were used as the input variables for the NN models, and the L3:CM1 charge was used as the output variable. The NN model results show that the model predictions are able to follow the actual L3:CM1 data, but with large fitting errors. This is because the most important factor, the kicker voltage, was ignored. The feature importance analysis by the random-forest-regressor [12] shows that the kicker voltage plays the most important role in changing the L3:CM1 charge, as shown in Fig. 2. The L3:CM1 charge is very sensitive to the kicker voltage, therefore, the kicker voltage is not included in the optimization input variables; instead, it held fixed during optimization and operation. However, the kicker voltage might be different for different operation shifts, so the input data is filtered for fixed kicker voltage, e.g., 13.5 kV.

Besides the 16 magnets used in the optimization, there are 12 other steering magnets located before L3:CM1 that are

Content from this work may be used under the terms of the CC BY 3.0 licence (© 2021). Any distribution of this work must maintain attribution to the author(s), title of the work, publisher, and DOI

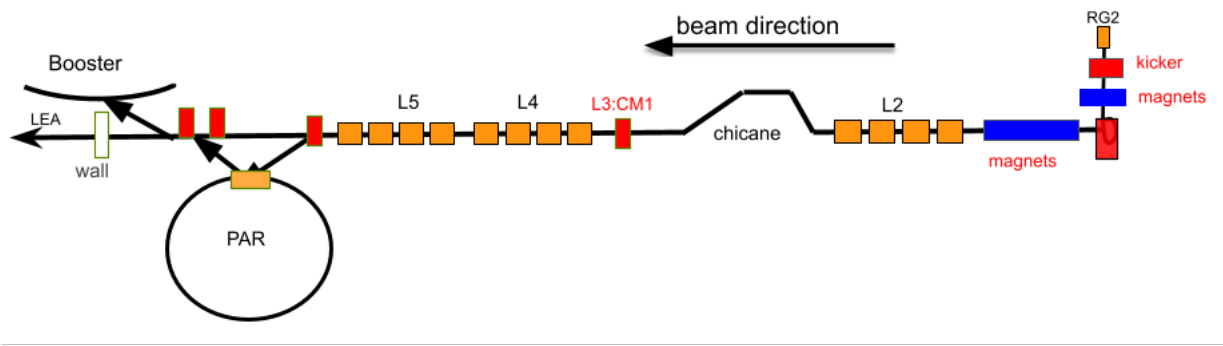


Figure 1: APS linac structure.

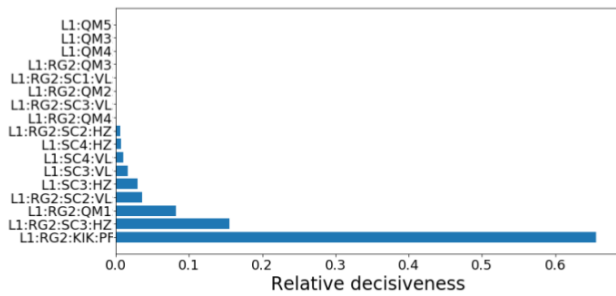


Figure 2: Importance analysis of 16 magnets and the kicker voltage by the random-forest-regressor.

continuously being adjusted by the feedback controller [13] so that the L3:CM1 charge is being changed by these 12 steering magnets accordingly. These 12 steering magnets were added to the input variables, so 28 input variables are being used for the NN model. Due to the slow response of the APS linac magnets, normally it takes about 10 seconds for a change of 0.4 Amps. However, the data logger logs at 4-second intervals, thus there are some data for the magnets' current (readback) that did not reach the setpoint. The input data is further cleaned by filtering the data where the readback and setpoint of the magnets do not agree within a tolerance of 0.05 A. In summary, the two-year archived data is being processed and cleaned as follows:

- extract data at a fixed kicker voltage of 13.5 kV.
- use all the magnets located before the L3:CM1 monitor as input variables.
- remove any data points where the readback and setpoint of the magnets do not agree within 0.05 A.

After applying the above processes, the input data has 13644 samples. The training, validation, and test set ratios for the NN models are set to 60%, 20%, and 20%, respectively.

RESULTS AND DISCUSSION

Figure 3 shows the prediction of the L3:CM1 charge for the three NN models versus the true values with the test set data. All three NN models are successful in predicting the

L3:CM1 values from the 28-magnet settings. The predictions for about 90% of the samples follow the true values well. However, there are large prediction errors when the L3:CM1 charge is around 0.5 nC and around 0.2 nC. After investigating, the large errors of the data points around 0.5 nC, seen in the top-middle of Fig. 3, come from the averaging problem when switching the kicker between on and off states. During APS top-up user operation [14], the L3:CM1 charge should be 0 when the injection is turned off or 1.0 nC (or more) when the injection is turned on. The log data is from the averaged L3:CM1 charge PV, which is averaged over the last two samples in the IOC. Sometimes when turning the kicker on for injection, the previous value of 0.0 nC is used for the average instead of using the value after the trigger is turned on, due to trigger timing jitters; therefore, the average value is about 0.5 nC instead of 1.0 nC. Using the non-averaged charge PV as output, these large errors caused by machine jitter disappear. However, due to the bigger noise level of the non-averaged charge, it has bigger prediction errors than the averaged charge overall. Thus, the averaged charge is being used in order to have cleaner input data.

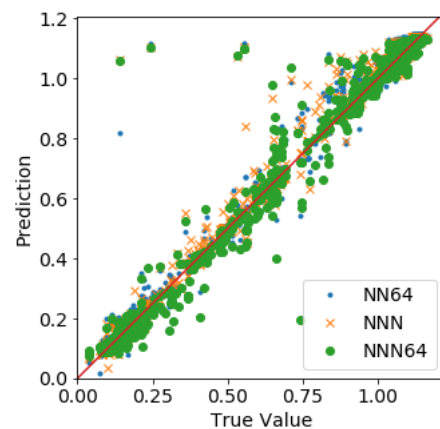


Figure 3: Predicted versus true values of the L3:CM1 charge for the three NN models.

The large errors around the 0.2-nC charge shown in the top-left of Fig. 3 are found to be caused by trajectory errors. Although the magnet settings are perfect for output above

the 1.0-nC L3:CM1 charge, the actual L3:CM1 charge is only about 0.2 nC due to a bad trajectory caused by the slow response of the steering feedback controller. This suggests that the abnormally large errors are not arbitrary, but actually give meaningful information that can be used to identify problems.

Figure 4 shows histograms of the absolute prediction errors of the three NN models. The mean absolute errors (MAEs) of NN64, NNN, and NNN64 are 0.0165, 0.0132, and 0.0151 nC, respectively. The NNN model turns out to have the smallest MAE. Since more than 90% of the data has a 1.0-nC charge, all NNN models are able to predict the L3:CM1 charge with about a 1 to 2% error from the 28-magnet settings.

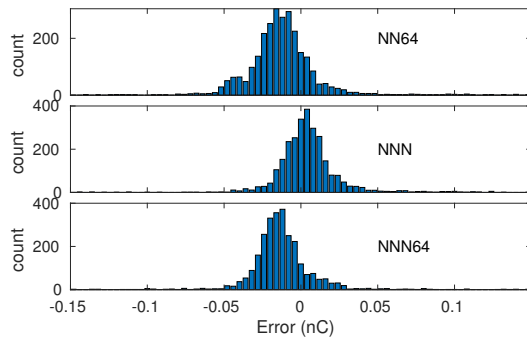


Figure 4: MAE histograms of the three NN models.

The NNN model that has different nodes in three hidden layers turns out to be the best NN model in the APS linac charge optimization application. However, it is impossible to test different combinations of the number of nodes and hidden layers manually.

While we looked for an optimizer to automatically find the best ML model for our application, we found an interesting tool, the Tree-based Pipeline Optimization Tool (TPOT) [15], which is a Python automated machine learning tool that optimizes machine learning pipelines using genetic programming. After running TPOT overnight with the same input data, a second-order polynomial-features regression model was found by TPOT. The predictions versus true values and the histogram of the prediction errors are shown in Fig. 5. The large prediction errors are from machine jitter and trajectory errors. The MAE of this second-order polynomial-features regression model is 0.0108 nC, slightly better than the NNN model. The first-order coefficients of the magnets also show that L1:RG2:QM2 and L1:RG2:SC2:HZ are the two most sensitive knobs. This second-order polynomial-features regression model is another option for APS linac charge optimization besides the NNN model.

SUMMARY

All three NN models are able to detect machine jitter and trajectory errors and to predict the L3:CM1 charge with about 1 to 2% error from the 28-magnet settings. The NNN model turns out to be the best and has the fewest number

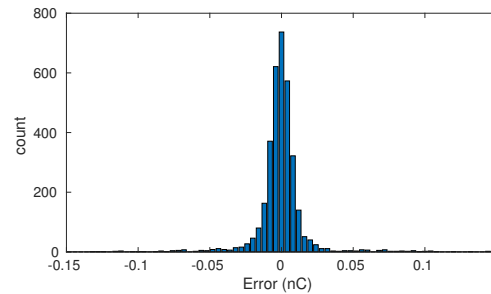
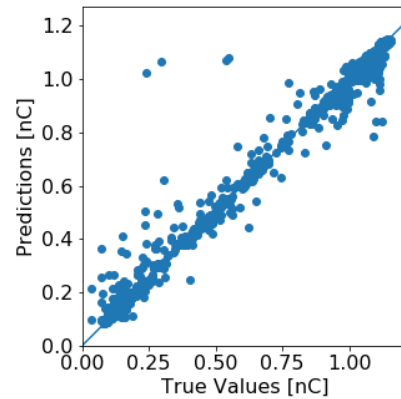


Figure 5: Results of second-order polynomial-features regression model: prediction vs. true value (top) and histogram of prediction error (bottom).

of MAE errors. From our experience with ML models, the quality of the data is important for ML model training. Input data should be examined to clean up machine jitter and/or trajectory errors before using them for developing ML models.

This important analysis of the ML models indicates that L1:RG2:QM2 and L1:RG2:SC2:HZ are the two most sensitive knobs in controlling beam lattice and trajectory. The settings of these two knobs have a strong impact on L3:CM1 charge and should be placed in the first two locations in the optimizer list to speed up the optimization process.

ACKNOWLEDGEMENTS

The authors would like to thank Michael Borland and Sasha Zholents at APS for helpful discussions on and their support of the ML studies.

REFERENCES

- [1] A. Edelen *et al.*, “Machine learning for orders of magnitude speedup in multiobjective optimization of particle accelerator systems”, *Physical Review Accelerators and Beams*, vol. 23, no. 4, Apr. 2020. doi:10.1103/physrevaccelbeams.23.044601
- [2] M. White *et al.*, “Status of the Advanced Photon Source (APS) Linear Accelerator”, in *Proc. 1994 Linear Accelerator Conf. (LINAC’94)*, Tsukuba, Japan, Aug. 1994, paper MO-62, pp. 208–210.

- [3] J. W. Lewellen *et al.*, “Operation of the APS RF Gun”, in *Proc. 19th Int. Linac Conf. (LINAC’98)*, Chicago, IL, USA, Aug. 1998, paper TH4042, pp. 863–865.
- [4] S. Shin, Y. Sun, and A. Zholents, “Interleaving Lattice Design for APS Linac”, in *Proc. North American Particle Accelerator Conf. (NAPAC’16)*, Chicago, IL, USA, Oct. 2016, pp. 713–715. doi:10.18429/JACoW-NAPAC2016-WEPOA12
- [5] Y. Sun *et al.*, “APS LINAC Interleaving Operation”, in *Proc. 10th Int. Particle Accelerator Conf. (IPAC’19)*, Melbourne, Australia, May 2019, pp. 1161–1163. doi:10.18429/JACoW-IPAC2019-MOPTS119
- [6] M. Borland *et al.*, “The Upgrade of the Advanced Photon Source”, in *Proc. 9th Int. Particle Accelerator Conf. (IPAC’18)*, Vancouver, Canada, Apr.-May 2018, pp. 2872–2877. doi:10.18429/JACoW-IPAC2018-THXGBD1
- [7] M. Borland, “Simulation of Swap-Out Reliability for the Advance Photon Source Upgrade”, in *Proc. North American Particle Accelerator Conf. (NAPAC’16)*, Chicago, IL, USA, Oct. 2016, pp. 881–883. doi:10.18429/JACoW-NAPAC2016-WEPOB02
- [8] W. B. Colson and A. M. Sessler, “Free electron lasers”, *Annu. Rev. Nucl. Part. Sci.*, vol. 35, pp. 25-54, 1985. doi:10.1146/annurev.ns.35.120185.000325
- [9] B. E. Carlsten and T. O. Raubenheimer, “Emittance growth of bunched beams in bends”, *Physical Review E*, vol. 51, no. 2, pp. 1453–1470, Feb. 1995. doi:10.1103/physreve.51.1453
- [10] M. Borland *et al.*, “Performance of the 2 MeV Microwave Gun for the SSRL 150 MeV Linac”, in *Proc. 1990 Linear Accelerator Conf. (LINAC’90)*, Albuquerque, NM, USA, Sep. 1990, paper TH461, pp. 761–763.
- [11] H. Shang, Y. Sun, and A. Hanuka, Private communication, 2019.
- [12] N. Donges, A complete guide to the random forest algorithm, <https://builtin.com/data-science/randomforest-algorithm>.
- [13] H. Shang, M. Borland, L. Emery, and R. Soliday, “New Features in the SDDS-Compliant EPICS ToolkitMicrosoft Word - FPAG004.doc”, in *Proc. 20th Particle Accelerator Conf. (PAC’03)*, Portland, OR, USA, May 2003, paper FPAG004, pp. 3470–3472.
- [14] L. Emery, “Recent Operational Data on Continuous Top-up Operation at the Advanced Photon Source”, in *Proc. 19th Particle Accelerator Conf. (PAC’01)*, Chicago, IL, USA, Jun. 2001, paper WPPH064, pp. 2599–2601.
- [15] EpistasisLab, <https://github.com/EpistasisLab/tpot>